A New Class of Biorthogonal Wavelet Systems for Image Transform Coding

Dong Wei, *Student Member, IEEE,* Jun Tian, Raymond O. Wells, Jr., and C. Sidney Burrus, *Fellow, IEEE*

***Abstract*—We construct general biorthogonal Coifman wavelet systems, a new class of compactly supported biorthogonal wavelet systems with vanishing moments equally distributed for a scaling function and wavelet pair. A time-domain design method is employed and closed-form expressions for the impulse responses and the frequency responses of the corresponding dual filters are derived. The resulting filter coefficients are all dyadic fractions, which is an attractive feature in the realization of multiplication-free discrete wavelet transform. Even-ordered systems in this family are symmetric, which correspond to linear-phase dual filters. In particular, three filterbanks (FB's) in this family are systematically verified to have competitive compression potential to the 9-7 tap biorthogonal wavelet FB by Cohen *et al*., which is currently the most widely used one in the field of wavelet transform coding. In addition, the proposed FB's have much smaller computational complexity in terms of floating-point operations required in transformation, and therefore indicate a better tradeoff between compression performance and computational complexity.**

***Index Terms*—Image coding, source coding, transform coding, wavelet transforms.**

I. Introduction

THE DISCRETE wavelet transform (DWT) has been applied extensively to digital image processing, especially transform coding of digital images and digital image sequences. Since images are mostly smooth (except for occasional edges), it seems appropriate that the wavelets should be reasonably smooth, which requires the associated filters to be long enough to obtain good smoothness and energy compaction capability. However, this will increase the computational cost of the corresponding transformation. On the other hand, it is desirable that the finite impulse response (FIR) filterbank (FB) be linear phase (corresponding to symmetry for wavelets and scaling functions). Unfortunately, it has been shown that orthogonality and symmetry are conflict properties for design of compactly supported nontrivial wavelets [1, p. 252, Th. 8.1.4]. The highly important linear phase constraint corresponding to symmetric wavelets may be maintained by relaxing the orthogonality constraint and using biorthogonal wavelet bases. Design of symmetric biorthogonal wavelet systems with their associated DWT having good compression potential and low computational complexity is an important issue in the area of wavelet transform coding.

Manuscript received December 13, 1995; revised December 9, 1996. This research was supported in part by Advanced Research Projects Agency, Texas Advanced Technology Program, and Texas Instruments, Inc. The associate editor coordinating the review of this manuscript and approving it for publication was Prof. C.-C. Jay Kuo.

D. Wei was with the Department of Electrical and Computer Engineering, Rice University, Houston, TX 77251-1892 USA. He is now with the Department of Electrical and Computer Engineering, University of Texas, Austin, TX 78712-1084 USA.

J. Tian and R. O. Wells, Jr., are with the Department of Mathematics, Rice University, Houston, TX 77251-1892 USA.

C. S. Burrus is with the Department of Electrical and Computer Engineering, Rice University, Houston, TX 77251-1892 USA (e-mail: csb@rice.edu).

Publisher Item Identifier S 1057-7149(98)04363-2.

A. Previous Work

Recently, biorthogonal wavelet systems[1] have been constructed [2]–[4]. In order to obtain reasonably smooth wavelets, Cohen *et al.* preassigned a number of vanishing moments on the two wavelets and determined the coefficients of the corresponding filters by factorizing trigonometric polynomials [2]. Several classes of symmetric and compactly supported biorthogonal wavelet systems (e.g., biorthogonal spline wavelet systems) were constructed by using their frequency-domain method. In [3], Vetterli and Herley constructed symmetric biorthogonal wavelet systems with vanishing moments imposed on wavelets using an FB-based approach. In [4], Phoong *et al*. proposed a framework for construction and implementation of a certain class of biorthogonal FB's that covers some causal stable infinite impulse response (IIR) FB's and some linear-phase FIR FB's. A general framework, a so-called *lifting scheme*, was proposed by Sweldens [5], which does not rely on spectral factorization and allows painless custom-design construction of biorthogonal wavelet systems. In addition, a *lifted fast biorthogonal wavelet transform* on this scheme was suggested in [5], which may be viewed as a generalization of the implementation proposed in [4].

The 9-7 tap biorthogonal wavelet FB (CDF-9-7 FB) designed in [2, Table 6.2] has become the most widely used wavelet system in the field of wavelet transform coding, and has been chosen as the only candidate FB in the FBI's fingerprint image compression standard [6]. In [7], several filter-based metrics are proposed to test the compression performance of over 4300 candidate FB's and the CDF-9-7 FB has turned out to be one of the best FB's for image compression. One major disadvantage of the CDF-9-7 FB lies in the fact that, because all the filter coefficients are irrational, the computational complexity of its associated DWT and inverse DWT (IDWT) is much higher than that of the DWT/IDWT using biorthogonal spline wavelet filters [2], whose coefficients are all dyadic fractions. In [8], a

[1] In this paper, we only consider two-band (or two-channel) biorthogonal wavelet systems possessing perfect reconstruction property.

multiplication-free DWT/IDWT algorithm using some short spline wavelet systems was proposed. However, in general the compression performance of the biorthogonal spline wavelet systems is worse than that of the CDF-9-7 FB. Therefore, in coding applications, choosing a wavelet system seems a tradeoff between compression performance and computational complexity.

In 1989, Coifman proposed the idea of constructing orthonormal wavelets with vanishing moments equally distributed for the scaling function and wavelet [9], [10]. Such wavelets, so called *coiflets*, were first constructed in [10] and later in [11] by different methods.

Let us consider the following two interesting observations: i) coiflets are closer to exact symmetric than the orthonormal Daubechies wavelets constructed in [12]; ii) some symmetric biorthogonal wavelets are very close to some coiflets [1, pp. 278–285], [2]. These observations may suggest that if we relax orthogonality and keep vanishing moments equally distributed for scaling function and wavelet it might be possible to obtain less asymmetric, or exactly symmetric, biorthogonal wavelet systems. In [11], a generalization of coiflets to the biorthogonal setting was introduced and a family of biorthogonal Coifman wavelet systems, parameterized by the same degree of moments for both two scaling functions and both two wavelets, was developed. In particular, the coefficients of the associated dual filters were all dyadic rational numbers with specific formulae for all orders. The maximally flat FIR linear-phase wavelet systems constructed in [4] are, in fact, the even-ordered biorthogonal Coifman wavelet systems. However, this was not explicitly pointed out in [4].

B. Aim of the Paper

In this paper, we generalize the biorthogonal Coifman wavelet systems from [11], $\{\phi, \psi, \tilde{\phi}, \tilde{\psi}\}$, to include a variable degree of vanishing moments for the wavelet ψ, say $\tilde{N}$, where the degrees of vanishing moments for the scaling function $\tilde{\phi}$ and the wavelet $\tilde{\psi}$ are the same and fixed (which turns out to fix the degree of vanishing moments of the scaling function ϕ as well), say N. We refer to these systems as *general biorthogonal Coifman wavelet systems* (GBCW systems), and the original biorthogonal Coifman wavelet systems of [11] with the same degree of vanishing moments for all four functions $(N = \tilde{N})$ are referred to as *strict biorthogonal Coifman wavelet systems*, an important special case of the general version. A time-domain design method is employed, which does not rely on spectral factorization, and is straightforward, because the vanishing moment conditions and the perfect reconstruction conditions can be translated into a set of linear conditions and a set of bilinear conditions on the associated dual filters, respectively, and the filter coefficients can be easily determined by solving simultaneous linear equations. We show that for any N and $\tilde{N}$ with the same parity, a unique solution exists. For the case $N \geq \tilde{N}$, closed-form expressions for the impulse responses and the frequency responses of the dual filters are derived. Even though we do not impose symmetry constraints in our construction, even-ordered members in this family are exactly symmetric.

It turns out that the GBCW systems are useful for image transform coding and seem to be quite comparable to the wavelet systems used in the state-of-the art image data compression systems. In particular, three GBCW FB's are shown to have competitive compression potential to the CDF-9-7 wavelet FB. They have not been applied to wavelet transform coding in the literature. We apply several filter-based metrics proposed in [7], including regularity, shift-variant impulse response, shift-variant step response, and weighted subband coding gain, to systematically compare the compression performance of the four wavelet FB's.

Moreover, due to the dyadic coefficients in the GBCW FB's, one can improve the implementation of the DWT/IDWT defined by these filters via replacing multiplications by additions in floating-point arithmetic in a systematic manner. Compared to the work in [8], we give a more general method to quickly compute the multiplications by dyadic fractions, which can be used for both the GBCW systems and the biorthogonal spline wavelet systems of any order. Though the increase in speed-up (from $O(M)$ to $O'(M)$ with a smaller constant for a length-M signal) is not as dramatic as the speed-up going from a discrete Fourier transform to a fast Fourier transform (from $O(M^2)$ to $O(M \log M)$), it may be useful in practice in terms of both software and hardware implementations. The resulting fast transformation is promising in those real-time applications where the data sets being processed are very large, e.g. digital video coding, fingerprint image compression.

Some of the wavelet systems reported by other researchers are related to our work. The synthesis filters of even-ordered GBCW systems have already been known in different forms in the literature [13]–[16]. After finishing this work, the authors realized some other results related to this work [5], [17], [18]. In [5], the whole family of even-ordered GBCW systems were constructed by lifting Donoho wavelets, and the moment property of scaling functions were explicitly pointed out. Some of the GBCW systems were discussed in terms of their construction and compression capability in [17, pp. 214–218, p. 249], and [18]. We shall provide more detailed discussions on the relation between these results and ours in the remaining of the paper as is appropriate.

Even though some of the systems constructed in our work have already been known, the novelty of this independent work lies in the following aspects:

- the construction scheme used in this work is quite different from those used in the aforementioned literature;
- the odd-ordered GBCW systems $(N > 1)$ can be constructed with the scheme, which form a new family to the best of our knowledge;
- for the case $N \geq \tilde{N}$ the explicit formulae for the analysis filters are novel;
- the systematic analysis of the compression potentials of three GBCW systems show that they are promising in transform coding applications.

C. Outline of the Paper and Notation

The remainder of the paper is organized as follows. In Section II, we introduce the concepts of general biorthogonal

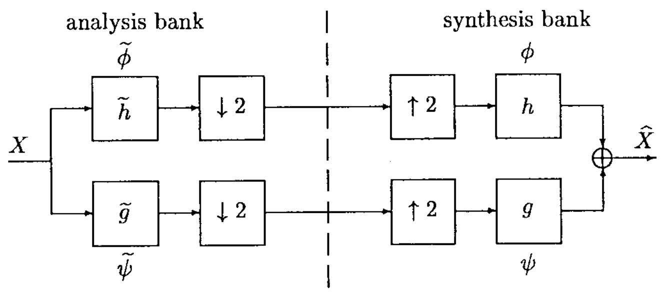

Fig. 1. Block diagram for a two-band biorthogonal FB and the associated wavelets and scaling functions ($g(n) = (-1)^n \tilde{h}(1-n), \tilde{g}(n) = (-1)^n h(1-n)$, and for a perfect reconstruction system $\hat{X} = X$).

Coifman wavelet systems, construct the associated dual filters, develop several interesting properties thereof, and formalize new arithmetic computational features for these new systems that speed up processing time. Also, we consider two special subclasses of GBCW systems in this section. In Section III, we present a systematic study of the compression abilities of three systems in this family in comparison with the CDF-9-7 systems. Section IV concludes the paper.

The following notation will be used in this paper. The symbols $\mathbb{R}$ and $\mathbb{Z}$ denote the set of real numbers and the set of integers, respectively. All integrals and summations without explicit limits indicate that the actual limits are $-\infty$ and $+\infty$. For any $t \in \mathbb{R}, \lfloor t \rfloor = \max\{s\colon s \in \mathbb{Z}, s \le t\}, \lceil t \rceil = \min\{s\colon s \in \mathbb{Z}, s \ge t\}$. The symbol δ_{mn} denotes Kronecker delta symbol, i.e., $\delta_{mn} = 1$ if and only if $m = n$. For a matrix $\boldsymbol{A}, \boldsymbol{A}^T$, and $\boldsymbol{A}^{-1}$, respectively, denote the transpose and inverse of $\boldsymbol{A}$.

II. General Biorthogonal Coifman Wavelet Systems

A. Problem Formulation

Let h and $\tilde{h}$ be the impulse responses of a pair of dual lowpass filters, respectively, the synthesis filter and the analysis filter, in a two-band biorthogonal FB (see Fig. 1). The associated scaling functions ϕ and $\tilde{\phi}$ are recursively defined as

$$\phi(x) = \sqrt{2} \sum_n h(n)\phi(2x-n) \tag{1}$$

and

$$\tilde{\phi}(x) = \sqrt{2} \sum_n \tilde{h}(n)\tilde{\phi}(2x-n). \tag{2}$$

The associated wavelets ψ and $\tilde{\psi}$ are defined as

$$\psi(x) = \sqrt{2} \sum_n (-1)^n \tilde{h}(1-n)\phi(2x-n) \tag{3}$$

and

$$\tilde{\psi}(x) = \sqrt{2} \sum_n (-1)^n h(1-n)\tilde{\phi}(2x-n). \tag{4}$$

Such a set of four functions, $\{\phi, \psi, \tilde{\phi}, \tilde{\psi}\}$, forms a two-band biorthogonal wavelet system. The perfect reconstruction condition is given by (see [2])

$$\sum_n h(n)\tilde{h}(n-2l) = \delta_{l0} \quad \forall l \tag{5}$$

or equivalently

$$H(\omega)\tilde{H}(-\omega) + H(\omega+\pi)\tilde{H}(-\omega+\pi) = 2 \tag{6}$$

where $H(\omega) = \Sigma_n h(n)e^{-jn\omega}$ and $\tilde{H}(\omega) = \Sigma_n \tilde{h}(n)e^{-jn\omega}$.

Definition 1: A biorthogonal wavelet system $\{\phi, \psi, \tilde{\phi}, \tilde{\psi}\}$ is a GBCW system of order N if the vanishing moments of one of the two function pairs, either $\{\phi, \psi\}$ or $\{\tilde{\phi}, \tilde{\psi}\}$, are of degree N. Without loss of generality, in the remainder of this paper we assume that in a GBCW system $\tilde{\phi}$ and $\tilde{\psi}$ satisfy

$$\int x^p \tilde{\phi}(x)\, dx = \delta_{p0} \quad \text{for } p = 0, 1, \cdots, N-1 \tag{7}$$

$$\int x^p \tilde{\psi}(x)\, dx = 0 \quad \text{for } p = 0, 1, \cdots, N-1. \tag{8}$$

From the above definition, we obtain the following lemma immediately.

Lemma 2: For a GBCW system of order $N, \{\phi, \psi, \tilde{\phi}, \tilde{\psi}\}$, the vanishing moments of ϕ are also of degree N, i.e.,

$$\int x^p \phi(x)\, dx = \delta_{p0} \quad \text{for } p = 0, 1, \cdots, N-1. \tag{9}$$

Proof: Using (2) and (4), one can show that the conditions (7) and (8) are equivalent to

$$\sum_n n^p \tilde{h}(n) = \sqrt{2}\delta_{p0} \quad \text{for } p = 0, 1, \cdots, N-1 \tag{10}$$

and

$$\sum_n (-1)^n n^p h(n) = 0 \quad \text{for } p = 0, 1, \cdots, N-1. \tag{11}$$

Therefore, we deduce that

$$\begin{aligned} \tilde{H}^{(p)}(0) &= \sqrt{2}\delta_{p0}, \\ H^{(p)}(\pi) &= 0 \quad \text{for } p = 0, 1, \cdots, N-1. \end{aligned} \tag{12}$$

For $p = 0, 1, \cdots, N$, taking the pth derivative on both sides of (6) and evaluating it at $\omega = 0$, we infer that $H^{(p)}(0) = \sqrt{2}\delta_{p0}$, or equivalently

$$\sum_n n^p h(n) = \sqrt{2}\delta_{p0} \quad \text{for } p = 0, 1, \cdots, N-1 \tag{13}$$

which implies that the vanishing moments of ϕ are also of degree N. □

Combining (11) and (13), we conclude that

$$\begin{aligned} \sum_m (2m)^p h(2m) &= \sum_m (2m+1)^p h(2m+1) \\ &= \frac{1}{\sqrt{2}}\delta_{p0} \quad \text{for } p = 0, 1, \cdots, N-1. \end{aligned} \tag{14}$$

Thus, we have translated the vanishing moment conditions on the scaling function $\tilde{\phi}$ and the wavelet $\tilde{\psi}$ in the definition of the GBCW system into a set of linear conditions on the dual filters h and $\tilde{h}$. In fact, using an argument similar to that in the above proof we can prove the following lemma.

Lemma 3: For a pair of dual filters h and $\tilde{h}$ in a biorthogonal wavelet system, if h satisfies the conditions (11) and (13), then $\tilde{h}$ satisfies the condition (10).

B. Construction of Synthesis Filter

1) Impulse Response: We construct the dual filters h and $\tilde{h}$ using the biorthogonality conditions (5) and the linear conditions (14) and (10). We first determine h using (14). We require h to have the minimal length among all filters satisfying (14), and denote the one associated with the Nth-order GBCW system by h_N. Since there are $2N$ independent conditions on h_N in (14), we define that h_N starts with $h_N(-N+1)$ and ends with $h_N(N)$. Note that these linear conditions on the filter coefficients naturally divides into two parts, on the even-indexed coefficients and on the odd-indexed coefficients. For the first part, it is easy to see the solution is exactly that

$$h_N(2m) = \delta_{m0}/\sqrt{2}. \tag{15}$$

For the second part, since the coefficient matrix of these simultaneous linear equations is a Vandermonde matrix, which is nonsingular, there is always a unique solution. The closed-form formulae for these odd-indexed coefficients are given by the following.

- If $N = 1$, then $h_1(2m+1) = \delta_{m0}/\sqrt{2}$.
- If $N = 2K, K = 1, 2, \cdots$, then for $-K \le m \le K-1$

$$h_{2K}(2m+1) = \frac{\prod_{k=-K, k\neq m}^{K-1}(2k+1)}{2^{2K+1/2}\prod_{k=-K, k\neq m}^{K-1}(k-m)} \tag{16}$$

$$= \frac{(-1)^m}{2m+1}\binom{2K-2}{K-1}\binom{2K-1}{K+m} \cdot \frac{2K-1}{2^{4K-5/2}}. \tag{17}$$

- If $N = 2K+1, K = 1, 2, \cdots$, then for $-K \le m \le K$

$$h_{2K+1}(2m+1) = \frac{\prod_{k=-K, k\neq m}^{K}(2k+1)}{2^{2K+3/2}\prod_{k=-K, k\neq m}^{K}(k-m)} \tag{18}$$

$$= \frac{(-1)^m}{2m+1}\binom{2K-1}{K-1}\binom{2K}{K+m} \cdot \frac{2K+1}{2^{4K-1/2}}. \tag{19}$$

From (15), it is easy to see that the actual length of h_N is $2N-1$ for $N>1$. In particular, the indices are from $-N+1$ to $N-1$ if N is even, and from $-N+2$ to N if N is odd. For a given order N such that $N>2$, while the synthesis filter in the Nth-order GBCW system is longer than the synthesis filter in the Nth-order biorthogonal spline wavelet system whose length is $N+1$, both of them have $N+1$ nonzero coefficients.

Filters satisfying (15) are commonly called *interpolating filters* or *à trous filters*, which are used in the *à trous algorithm* to quickly compute samples of a continuous wavelet transform [15], [19].

2) Frequency Response: From (15), (17), and (19), we deduce that the frequency response of the filter h_N is given by the following.

- If $N = 2K, K = 1, 2, \cdots$, then

$$H_{2K}(\omega) = \sqrt{2}\left(\cos\left(\frac{\omega}{2}\right)\right)^{2K}\sum_{k=0}^{K-1}\binom{K-1+k}{k} \cdot \left(\sin\left(\frac{\omega}{2}\right)\right)^{2K}. \tag{20}$$

- If $N = 2K-1, K = 1, 2, \cdots$, then

$$H_{2K-1}(\omega) = H_{2K}(\omega) + jH_{2K}^{(1)}(\omega)/(2K-1). \tag{21}$$

Since $(\cos(\omega/2))^2 = (2+e^{j\omega}+e^{-j\omega})/4$ and $(\sin(\omega/2))^2 = (2-e^{j\omega}-e^{-j\omega})/4$, we conclude from (20) that the coefficients of h_{2K} are all dyadic fractions (we ignore the normalizing factor $\sqrt{2}$). From (17), we know that the coefficients of the polynomial (in terms of $e^{j\omega}$) $H_{2K}^{(1)}(\omega)/(2K-1)$ are all dyadic fractions. Therefore, according to (21) the coefficients of h_{2K+1} are all dyadic fractions.

3) Interpolating Scaling Functions: A scaling function ϕ is *interpolating* or *cardinal* if $\phi(n) = \delta_{n0}$ for all $n \in \mathbb{Z}$. The advantage of using interpolating scaling functions is that the interpolatory reconstruction of a function $f, \tilde{f}(t) = \Sigma_n f(2^{-J}n)\phi(2^J t - n)$, satisfies that $\tilde{f}(2^{-J}n) = f(2^{-J}n)$ for all $n \in \mathbb{Z}$. The synthesis scaling functions of even-ordered GBCW systems are known to be interpolating [5]. Applying Th. 10 in [5] and using (21) one can verify that the synthesis scaling functions of odd-ordered GBCW systems are also interpolating.

4) Symmetry: For a lowpass filter h, there are two types of symmetry: (a) *whole-point symmetric* (WPS), i.e., $h(n) = h(2n_0 - n)$ for some constant $n_0 \in \mathbb{Z}$ and $\forall n$; (b) *half-point symmetric* (HPS), i.e., $h(n) = h(2n_0+1-n)$ for some constant $n_0 \in \mathbb{Z}$ and $\forall n$. From (15), (17), and (19), it is clear that h_N is WPS about the origin, i.e., $h_N(n) = h_N(-n)$, if and only if N is even. A question naturally arises: can one construct some "new" h_N by increasing the length of h_N to obtain more degrees of freedom so that the resulting filters are: i) HPS; ii) WPS for odd N? The following two lemmas provides the answer.

Lemma 4: For a GBCW system of order N, h_N cannot be HPS if $N > 0$.

Proof: If $h_N(n) = h_N(2n_0 + 1 - n)$ and $N > 0$, then according to (14)

$$\begin{aligned}\sum_m (2m+1)h_N(2m+1) &= \sum_m (2m)h_N(2n_0 - 2m) + \sum_m h_N(2m+1) \quad (22)\\ &= (2n_0+1)/\sqrt{2} \quad (23)\end{aligned}$$

which cannot be zero and is conflict with (14). □

Lemma 5: For a GBCW system of order N, h_N cannot be WPS if N is odd.

Proof: If $h_N(n) = h_N(2n_0 - n)$ and N is odd, then using (11) we deduce that

$$\begin{aligned}\sum_n (-1)^n n^N h_N(n) &= \sum_n (-1)^n n^N h_N(2n_0 - n) \quad (24)\\ &= \sum_n \sum_{l=0}^{N} \binom{N}{l} (-1)^{n+l}(2n_0)^{N-l} n^l h_N(n) \quad (25)\\ &= -\sum_n (-1)^n n^N h_N(n) \quad (26)\end{aligned}$$

which implies $\Sigma_n (-1)^n n^N h_N(n) = 0$ and is conflict with the assumption that the degree of vanishing moments is N. □

5) Relation to Other Results in the Literature: The synthesis filters of the even-ordered GBCW systems have already been known in different forms in the literature. They are called *Deslauriers-Dubuc filters* because Deslauriers and Dubuc first used them in the context of interpolating subdivision for construction of smooth curves [13]. In [14], Ansari *et al*. called these filters *Lagrangian halfband filters* because they are halfband and can be constructed using Lagrangian interpolation, and show that both the orthogonal Daubechies filters and the biorthogonal spline wavelet filters as well as their variations (e.g., the CDF-9-7 system) can be derived from these filters using spectral factorization. These filters can also be found as autocorrelation functions of the orthogonal Daubechies filters [15], [16]. In addition, these filters are discussed in the recent textbook by Strang and Nguyen [17, pp. 214–218].

C. Construction of Analysis Filter

1) Impulse Response:

Lemma 6: Assume that for a GBCW system of order N, the lengths of h and $\tilde{h}$ are L and $\tilde{L}$, respectively. Then L and $\tilde{L}$ satisfy

$$\tilde{L} - L = \begin{cases} 4l - 4, & l \in \mathbb{Z}, \quad \text{if } N \text{ is odd;} \\ 4l - 2, & l \in \mathbb{Z}, \quad \text{if } N \text{ is even.} \end{cases} \quad (27)$$

Lemma 6 can be proved by using (5) and the fact that $L = 2N - 1$.

For a given filter h_N, (5) gives $(\tilde{L} + L - 2)/2$ linear conditions on the filter $\tilde{h}$. According to Lemma 3, the conditions (10) are automatically satisfied by $\tilde{h}$. Hence, there are $(\tilde{L} - L + 2)/2$ degrees of freedom. According to Lemma 6, there is at least one degree of freedom in determining $\tilde{h}$. In our method, we use all the remaining degrees of freedom to maximize the number of vanishing moments of ψ, or equivalently, to maximize $\tilde{N}$ such that

$$\sum_n (-1)^n n^p \tilde{h}(n) = 0 \quad \text{for } p = 0, 1, \cdots, \tilde{N} - 1. \quad (28)$$

We denote such a filter by $\tilde{h}_{N,\tilde{N}}$. We set $\tilde{N} = (\tilde{L} - L + 2)/2$, and thus we infer that $\tilde{L} = 2N + 2\tilde{N} - 3$ and $\tilde{L} \geq L$. Assume that $\tilde{h}_{N,\tilde{N}}$ starts with $\tilde{h}_{N,\tilde{N}}(-N - \tilde{N} + 2)$ and ends with $\tilde{h}_{N,\tilde{N}}(N + \tilde{N} - 2)$. We attempt to solve (5) and (28), a total of $\tilde{L}$ simultaneous linear equations, to determine the coefficients of $\tilde{h}_{N,\tilde{N}}$. From Lemma 6, we know that $\tilde{N}$ and N have the same parity.

Using (15), we can rewrite the $N + \tilde{N} - 1$ equations in (5), which all contain some explicit terms of even-indexed coefficients, as, for $m = (-N - \tilde{N} + 2)/2, (-N - \tilde{N} + 4)/2, \cdots, (N + \tilde{N} - 2)/2$

$$\tilde{h}_{N,\tilde{N}}(2m) = \sqrt{2}\left(\delta_{m0} - \sum_l \tilde{h}_{N,\tilde{N}}(2l+1)h_N(2l+1-2m)\right) \quad (29)$$

which implies that the $N + \tilde{N} - 1$ even-indexed coefficients of $\tilde{h}_{N,\tilde{N}}$ can be uniquely determined by the odd-indexed coefficients of h_N and $\tilde{h}_{N,\tilde{N}}$ with the above $N + \tilde{N} - 1$ equations. Hence, we intend to determine the odd-indexed coefficients first. For any impulse response h, we define $\mathcal{M}_k[h] = \Sigma_m (2m+1)^k h(2m+1)$. We use (29) to rewrite the left-hand side of (28) as

$$\begin{aligned}\sum_n (-1)^n n^p \tilde{h}_{N,\tilde{N}}(n) &= \sum_m (2m)^p \tilde{h}_{N,\tilde{N}}(2m) - \mathcal{M}_p[\tilde{h}_{N,\tilde{N}}] \quad (30)\\ &= \sqrt{2}\sum_m (2m)^p \left(\delta_{m0} - \sum_l \tilde{h}_{N,\tilde{N}}(2l+1) \cdot h_N(2l+1-2m)\right) - \mathcal{M}_p[\tilde{h}_{N,\tilde{N}}] \quad (31)\\ &= \sqrt{2}\delta_{p0} - \mathcal{M}_p[\tilde{h}_{N,\tilde{N}}] - \sqrt{2}\sum_m \sum_l \cdot ((2l+1) - (2l+1-2m))^p h_N(2l+1-2m) \cdot \tilde{h}_{N,\tilde{N}}(2l+1) \quad (32)\\ &= \sqrt{2}\delta_{p0} - 2\mathcal{M}_p[\tilde{h}_{N,\tilde{N}}] - \sqrt{2}\sum_{k=0}^{p-1}\binom{p}{k}(-1)^{p-k} \cdot \mathcal{M}_{p-k}[h_N]\mathcal{M}_k[\tilde{h}_{N,\tilde{N}}] \quad (33)\end{aligned}$$

for $p = 0, 1, \cdots, \tilde{N} - 1$. Therefore, if $N \geq 2$, then we can determine the $N + \tilde{N} - 2$ odd-indexed coefficients by solving a total of $N + \tilde{N} - 2$ simultaneous linear equations, i.e., $N - 2$ equations without explicit terms of those even-indexed coefficients from (5) and $\tilde{N}$ equations from (28) using the above rewritten forms. Next, we discuss how to solve these linear equations for two cases $\tilde{N} \leq N$ and $\tilde{N} > N$.

a) The case $\tilde{N} \le N$: Due to (14), (29) becomes $\mathcal{M}_p[\tilde{h}_{N,\tilde{N}}] = \delta_{p0}/\sqrt{2}$, for $p = 0, 1, \cdots, \tilde{N}-1$. We write these equations and those from (5) using a matrix format, $\boldsymbol{Ah} = \boldsymbol{b}$, or

$$\begin{bmatrix} \boldsymbol{A}_{11} & \boldsymbol{A}_{12} & \boldsymbol{A}_{13} \\ \boldsymbol{A}_{21} & \boldsymbol{A}_{22} & \boldsymbol{A}_{23} \\ \boldsymbol{A}_{31} & \boldsymbol{A}_{32} & \boldsymbol{A}_{33} \end{bmatrix} \begin{bmatrix} \tilde{h}_{N,\tilde{N}}(-N-\tilde{N}+3) \\ \tilde{h}_{N,\tilde{N}}(-N-\tilde{N}+5) \\ \vdots \\ \tilde{h}_{N,\tilde{N}}(N+\tilde{N}-3) \end{bmatrix} = \begin{bmatrix} \boldsymbol{b}_1 \\ \boldsymbol{b}_2 \\ \boldsymbol{b}_3 \end{bmatrix} \tag{34}$$

where $\boldsymbol{A}_{11}$ and $\boldsymbol{A}_{33}$ are a $(\lceil N/2 \rceil - 1) \times (\lceil N/2 \rceil - 1)$ lower-triangle matrix and a $(\lfloor N/2 \rfloor - 1) \times (\lfloor N/2 \rfloor - 1)$ upper-triangle matrix, respectively, as in (35) and (36), shown at the bottom of the page. The matrix $\boldsymbol{A}_{22}$ is an $\tilde{N} \times \tilde{N}$ Vandermonde matrix, (37), shown at the bottom of the next page; the matrices $\boldsymbol{A}_{12}, \boldsymbol{A}_{13}, \boldsymbol{A}_{31}$, and $\boldsymbol{A}_{32}$ are zero matrices of proper sizes; the vectors $\boldsymbol{b}_1$ and $\boldsymbol{b}_3$ are zero vectors of lengths $\lceil N/2 \rceil - 1$ and $\lfloor N/2 \rfloor - 1$, respectively; $\boldsymbol{b}_2$ is a vector of length $\tilde{N}$, and is given by $\boldsymbol{b}_2 = [(1/\sqrt{2}) \quad 0 \quad 0 \quad \cdots \quad 0]^T$.

Since the determinant of $\boldsymbol{A}$ is the product of the determinants of $\boldsymbol{A}_{11}, \boldsymbol{A}_{22}$, and $\boldsymbol{A}_{33}$, which are all nonsingular matrices, the matrix $\boldsymbol{A}$ is also nonsingular. Thus, there always exists a unique solution $\boldsymbol{h} = \boldsymbol{A}^{-1}\boldsymbol{b}$. We here give the formulae for all the nonzero odd-indexed coefficients of $\tilde{h}_{N,\tilde{N}}$ in three cases, as follows.

- If $\tilde{N} = 1$, then $\tilde{h}_{N,\tilde{N}}(2m+1) = \delta_{m0}/\sqrt{2}$.
- If $\tilde{N} = 2\tilde{K}, \tilde{K} = 1, 2, \cdots$, then for $-\tilde{K} \le m \le \tilde{K}-1$
$$\tilde{h}_{N,\tilde{N}}(2m+1) = \frac{(-1)^m}{2m+1} \binom{2\tilde{K}-2}{\tilde{K}-1} \binom{2\tilde{K}-1}{\tilde{K}+m} \frac{2\tilde{K}-1}{2^{4\tilde{K}-5/2}}. \tag{38}$$
- If $\tilde{N} = 2\tilde{K}+1, \tilde{K} = 1, 2, \cdots$, then for $-\tilde{K} \le m \le \tilde{K}$
$$\tilde{h}_{N,\tilde{N}}(2m+1) = \frac{(-1)^m}{2m+1} \binom{2\tilde{K}-1}{\tilde{K}-1} \binom{2\tilde{K}}{\tilde{K}+m} \frac{2\tilde{K}+1}{2^{4\tilde{K}-1/2}}. \tag{39}$$

We observe that, because the matrix $\boldsymbol{A}_{22}$ only depends on $\tilde{N}$, the odd-indexed coefficients of $\tilde{h}_{N,\tilde{N}}$ only depends on $\tilde{N}$, too. Furthermore, by comparing (17) and (19) with (38) and (39), we conclude that if $\tilde{N} \le N$, then

$$\tilde{h}_{N,\tilde{N}}(2m+1) = h_{\tilde{N}}(2m+1) \quad \forall m. \tag{40}$$

Since we have known that for any $\tilde{N}$ the coefficients of $h_{\tilde{N}}$ are all dyadic fractions, from (40) and (29) we conclude that the coefficients of $\tilde{h}_{N,\tilde{N}}$ are all dyadic fractions as well.

b) The case $\tilde{N} > N$: The structure of those simultaneous linear equations is more involved for this case. We use an indirect approach that is similar to the one used in [5, Sect. 8.2]. In fact, (33) provides a way to recursively calculate $\mathcal{M}_p[\tilde{h}_{N,\tilde{N}}]$:

$$\mathcal{M}_p[\tilde{h}_{N,\tilde{N}}] = -\frac{1}{\sqrt{2}} \sum_{k=0}^{p-1} \binom{p}{k} (-1)^{p-k} \mathcal{M}_{p-k}[h_N] \cdot \mathcal{M}_k[\tilde{h}_{N,\tilde{N}}] \quad \text{for } p = 1, 2, \cdots, \tilde{N}-1 \tag{41}$$

where $\mathcal{M}_0[\tilde{h}_{N,\tilde{N}}] = 1/\sqrt{2}$. Now we can write equations $\Sigma_m (2m+1)^p \tilde{h}_{N,\tilde{N}}(2m+1) = \mathcal{M}_p[\tilde{h}_{N,\tilde{N}}]$, for $p = 0, 1, \cdots, \tilde{N}-1$, and those from (5) using a matrix format, $\boldsymbol{Ah} = \tilde{\boldsymbol{b}}$, where the vector $\tilde{\boldsymbol{b}}$ is given by

$$\begin{aligned} \tilde{\boldsymbol{b}} &= [\tilde{\boldsymbol{b}}_1^T \quad \tilde{\boldsymbol{b}}_2^T \quad \tilde{\boldsymbol{b}}_3^T]^T \\ &= [\tilde{\boldsymbol{b}}_1^T \mathcal{M}_0[\tilde{h}_{N,\tilde{N}}] \quad \mathcal{M}_1[\tilde{h}_{N,\tilde{N}}] \quad \cdots \quad \mathcal{M}_{\tilde{N}-1}[\tilde{h}_{N,\tilde{N}}] \\ &\qquad \tilde{\boldsymbol{b}}_3^T]^T. \end{aligned} \tag{42}$$

$\tilde{\boldsymbol{b}}_1$ and $\tilde{\boldsymbol{b}}_3$ are zero vectors of lengths $\lceil N/2 \rceil - 1$ and $\lfloor N/2 \rfloor - 1$, respectively, and, $\boldsymbol{A}$ and $\boldsymbol{h}$ are the same as those given for the case $\tilde{N} \le N$. Therefore, there always exists a unique solution $\boldsymbol{h} = \boldsymbol{A}^{-1}\tilde{\boldsymbol{b}}$ for this case, though its closed form could be quite complicated.

From the above discussion, it is easy to see that the actual length of $\tilde{h}_{N,\tilde{N}}$ is $2(N+\tilde{N})-3$ for $N > 1$. In particular, the

$$\boldsymbol{A}_{11} = \begin{cases} \begin{bmatrix} h_N(N-1) & 0 & 0 & \cdots & 0 \\ h_N(N-3) & h_N(N-1) & 0 & \cdots & 0 \\ \vdots & \vdots & & & \\ h_N(3) & h_N(5) & h_N(7) & \cdots & h_N(N-1) \end{bmatrix} & \text{for } N \text{ is even} \\ \begin{bmatrix} h_N(N) & 0 & 0 & \cdots & 0 \\ h_N(N-2) & h_N(N) & 0 & \cdots & 0 \\ \vdots & \vdots & & & \\ h_N(3) & h_N(5) & h_N(7) & \cdots & h_N(N) \end{bmatrix} & \text{for } N \text{ is odd} \end{cases} \tag{35}$$

$$\boldsymbol{A}_{33} = \begin{cases} \begin{bmatrix} h_N(-N+1) & h_N(-N+3) & \cdots & h_N(-5) & h_N(-3) \\ 0 & h_N(-N+1) & \cdots & h_N(-7) & h_N(-5) \\ \vdots & & & & \vdots \\ 0 & 0 & \cdots & 0 & h_N(-N+1) \end{bmatrix} & \text{for } N \text{ is even} \\ \begin{bmatrix} h_N(-N+2) & h_N(-N+4) & \cdots & h_N(-5) & h_N(-3) \\ 0 & h_N(-N+2) & \cdots & h_N(-7) & h_N(-5) \\ \vdots & & & & \vdots \\ 0 & 0 & \cdots & 0 & h_N(-N+2) \end{bmatrix} & \text{for } N \text{ is odd} \end{cases} \tag{36}$$

indices are from $-N-\tilde{N}+2$ to $N+\tilde{N}-2$. For given N and $\tilde{N}$ such that $N>2$, while the analysis filter in the Nth-order GBCW system is longer than the analysis filter in the Nth-order biorthogonal spline wavelet system whose length is $N+2\tilde{N}-1$, both of them have $N+2\tilde{N}-1$ nonzero coefficients.

2) Frequency Response: Using (40), (29), and (15), we infer that if $\tilde{N} \le N$, then

$$\begin{aligned}\tilde{H}_{N,\tilde{N}}(\omega) &= \sum_m \tilde{h}_{N,\tilde{N}}(2m+1)e^{-j(2m+1)\omega} \\ &\quad + \sum_m \tilde{h}_{N,\tilde{N}}(2m)e^{-j2m\omega} \qquad (43)\\ &= \sum_m h_{\tilde{N}}(2m+1)e^{-j(2m+1)\omega} \\ &\quad + \sqrt{2}\sum_m \Bigg(\delta_{m0} - \sum_l h_{\tilde{N}}(2l+1) \\ &\quad \cdot h_N(2l+1-2m)\Bigg)e^{-j2m\omega} \qquad (44)\\ &= H_{\tilde{N}}(\omega) + \frac{1}{\sqrt{2}} - \sqrt{2}\left(H_N(-\omega) - \frac{1}{\sqrt{2}}\right) \\ &\quad \cdot \left(H_{\tilde{N}}(\omega) - \frac{1}{\sqrt{2}}\right) \qquad (45)\end{aligned}$$

i.e.,

$$\tilde{H}_{N,\tilde{N}}(\omega) = 2H_{\tilde{N}}(\omega) + H_N(-\omega) - \sqrt{2}H_{\tilde{N}}(\omega)H_N(-\omega). \qquad (46)$$

3) Symmetry: If $h_N(n) = h_N(-n)$ and $\tilde{h}_{N,\tilde{N}}(n)$ is the unique solution for a given $\tilde{N}$, then $\tilde{h}_{N,\tilde{N}}(-n)$ also satisfies (5) and (28). This implies that $\tilde{h}_{N,\tilde{N}}(n) = \tilde{h}_{N,\tilde{N}}(-n)$ if and only if N is even. Hence, even though we do *not* impose the symmetry constraints in our construction, half the members in the family of GBCW systems are exactly symmetric.

D. Multiplication-Free DWT/IDWT

One remarkable property of h_N and $\tilde{h}_{N,\tilde{N}}$ is that all the filter coefficients are dyadic fractions multiplied by a normalizing factor $\sqrt{2}$. This property can be used to reduce computational cost of DWT/IDWT in the sense that it can lead to a multiplication-free DWT/IDWT. For the numbers in IEEE standard floating-point format, the multiplication by 2^b can be implemented as the addition of b to the exponent, while for integers only a shift operation is needed.[2] In addition, for any dyadic fraction of the form $2^b(2a+1), a, b \in \mathbb{Z}$, there exists a set $\tilde{\mathbb{Z}}, \tilde{\mathbb{Z}} \subset \mathbb{Z}$, such that $\tilde{\mathbb{Z}}$ has at most $\lceil \log_2 |2a+1| \rceil$ elements, and $2^b(2a+1) = \Sigma_{k\in\tilde{\mathbb{Z}}} 2^k$. Therefore, multiplication by a dyadic fraction can be implemented as summations of some weighted versions of the original number with all weights having the form 2^k. If the dyadic fraction is very close to some dyadic number, 2^k, for some k, then the size of $\tilde{\mathbb{Z}}$ will be very small.

Another useful property, which is not possessed by the biorthogonal spline wavelet systems and some other biorthogonal wavelet systems, is that nearly half of the coefficients of $\tilde{h}_N$ and some of the coefficients of $\tilde{h}_{N,\tilde{N}}$ are zero-valued. This considerably reduces the computational cost of filtering in the DWT/IDWT.

E. Relation to Other Results in the Literature

We list in Table I the coefficients of the dual filters h_N and $\tilde{h}_{N,\tilde{N}}$ for some small N and $\tilde{N}$. Using the criterion developed in [11], it is easy to check that for the GBCW systems in Table I, ψ and $\tilde{\psi}$ do constitute dual Riesz bases. Note that the GBCW systems of orders 1 and 2 happen to be the same as the biorthogonal spline wavelets with $N=1$ and $N=2$ in [2, Table 6.1], respectively. The even-ordered GBCW systems have been constructed using the lifting scheme in [5]. In addition, the moment property of scaling functions and the uniqueness of solutions were explicitly pointed out there. A fast wavelet transform algorithm based on the lifting scheme was proposed in [5]. It emerged from an interesting viewpoint of system structure, which is quite different from our arithmetic-based one. However, with our scheme we can construct both the even-ordered and the odd-ordered GBCW systems and derive the explicit formulae for $\tilde{h}_{N,\tilde{N}}$ and $\tilde{H}_{N,\tilde{N}}$ for the case $N \ge \tilde{N}$.

F. Minimum-Length Biorthogonal Coifman Wavelet Systems

In this subsection we consider one special class of the GBCW systems, in which ψ has the minimum degree of the vanishing moments for a given degree of vanishing moments for $\tilde{\phi}$ and $\tilde{\psi}$.

Definition 7: A GBCW system of order N is called a *minimum-length biorthogonal Coifman wavelet* system (ML-

[2] The normalizing factor $\sqrt{2}$ can be ignored in the implementation of the DWT/IDWT by scaling the analysis filters and the synthesis filters by factors of $\sqrt{2}$ and $1/\sqrt{2}$, respectively, or vice versa, so that perfect reconstruction is maintained.

$$\boldsymbol{A}_{22} = \begin{cases} \begin{bmatrix} 1 & 1 & \cdots & 1 \\ 1-\tilde{N} & 3-\tilde{N} & \cdots & -1+\tilde{N} \\ \vdots & \vdots & & \vdots \\ (1-\tilde{N})^{\tilde{N}-1} & (3-\tilde{N})^{\tilde{N}-1} & \cdots & (-1+\tilde{N})^{\tilde{N}-1} \end{bmatrix} & \text{for } N \text{ is even} \\ \begin{bmatrix} 1 & 1 & \cdots & 1 \\ 2-\tilde{N} & 4-\tilde{N} & \cdots & \tilde{N} \\ \vdots & \vdots & & \vdots \\ (2-\tilde{N})^{\tilde{N}-1} & (4-\tilde{N})^{\tilde{N}-1} & \cdots & \tilde{N}^{\tilde{N}-1} \end{bmatrix} & \text{for } N \text{ is odd} \end{cases} \qquad (37)$$

TABLE I
COEFFICIENTS OF h_N AND $\tilde{h}_{N,\tilde{N}}$, RESPECTIVELY, GIVEN BY $H_N(\omega)$ AND $\tilde{H}_{N,\tilde{N}}(\omega)$ WITH RESPECT TO $z = e^{-j\omega}$ (FOR SOME VERY LONG FILTERS. WE ONLY LIST HALF THE COEFFICIENTS AND THE OTHER CAN BE DEDUCED BY SYMMETRY)

N	$\sqrt{2}H_N(\omega)$	$\tilde{N}$	$\sqrt{2}\tilde{H}_{N,\tilde{N}}(\omega)$
1	$1+z$	1	$1+z$
		3	$2^{-3}(-z^{-2}+z^{-1}+8+8z+z^2-z^3)$
2	$2^{-1}(z^{-1}+2+z)$	2	$2^{-2}(-z^{-2}+2z^{-1}+6+2z-z^2)$
		4	$2^{-6}(3z^{-4}-6z^{-3}-16z^{-2}+38z^{-1}$ $+90+38z-16z^2-6z^3+3z^4)$
3	$2^{-3}(3z^{-1}+8+6z-z^3)$	1	$2^{-3}(z^{-2}+10+8z-3z^2)$
		3	$2^{-6}(3z^{-4}-12z^{-2}+24z^{-1}+82$ $+48z-12z^2-8z^3+3z^4)$
4	$2^{-4}(-z^{-3}+9z^{-1}+16+9z-z^3)$	2	$2^{-5}(z^{-4}-8z^{-2}+16z^{-1}+46$ $+16z-8z^2+z^4)$
		4	$2^{-8}(-z^{-6}+18z^{-4}-16z^{-3}-63z^{-2}$ $+144z^{-1}+348+144z+\cdots)$
		6	$2^{-13}(9z^{-8}-140z^{-6}+144z^{-5}$ $+756z^{-4}-944z^{-3}-1908z^{-2}$ $+4896z^{-1}+10758+4896z+\cdots)$
5	$2^{-7}(-5z^{-3}+60z^{-1}+128+90z$ $-20z^3+3z^5)$	1	$2^{-7}(-3z^{-4}+20z^{-2}+166$ $+128z-60z^2+5z^4)$
		3	$2^{-10}(-9z^{-6}+42z^{-4}-147z^{-2}$ $+384z^{-1}+1308+768z-255z^2$ $-128z^3+90z^4-5z^6)$
		5	$2^{-14}(15z^{-8}-280z^{-6}+1380z^{-4}$ $-640z^{-3}-3240z^{-2}+7680z^{-1}+20634$ $+11520z^1-3240z^2-2560z^3+1380z^4$ $+384z^5-280z^6+15z^8)$
6	$2^{-8}(3z^{-5}-25z^{-3}+150z^{-1}$ $+256+150z-25z^3+3z^5)$	2	$2^{-9}(-3z^{-6}+22z^{-4}-125z^{-2}$ $+256z^{-1}+724+256z+\cdots)$
		4	$2^{-12}(3z^{-8}-52z^{-6}+348z^{-4}$ $-256z^{-3}-972z^{-2}+2304z^{-1}$ $+5442+2304z+\cdots)$
		6	$2^{-16}(-9z^{-10}+150z^{-8}-1525z^{-6}$ $+768z^{-5}+6600z^{-4}-6400z^{-3}-14850z^{-2}$ $+38400z^{-1}+84804+38400z+\cdots)$

TABLE II
COMPARISON USING IMAGE-INDEPENDENT MEASURES

Test FBs	Regularity		MPSR	APSR	MFOSS	AFOSS
	$h_{N,\tilde{N}}$	h_N				
CDF-9-7	1.00	1.70	11.22	13.93	0.0411	0.0271
GBCW-9-7	0.15	2.00	9.79	18.67	0.0351	0.0194
GBCW-13-7	0.85	2.00	10.67	15.05	0.0379	0.0263
GBCW-13-11	0.20	2.82	9.34	18.64	0.0418	0.0291

TABLE III
COMPARISON USING THE WEIGHTED SBC GAIN

Test FBs	Lenna	Peppers	Boats	Building	Fingerprint-1	Fingerprint-2
CDF-9-7	49.29	32.12	37.96	28.36	77.40	46.60
GBCW-9-7	48.61	31.60	39.48	27.76	86.18	52.31
GBCW-13-7	50.34	32.79	40.94	28.74	88.72	53.89
GBCW-13-11	48.24	31.10	38.47	27.76	89.11	54.92

BCW system) of order N if the vanishing moments of ψ are of degree 1 for N is odd, and of degree 2 for N is even.

For an Nth-order MLBCW system, the length of $\tilde{h}_{N,1}$ (or $\tilde{h}_{N,2}$) is the minimum among all possible lengths of $\tilde{h}_{N,\tilde{N}}$. According to Lemma 6, if N is odd, then $\tilde{L} = L$; if N is odd, then $\tilde{L} = L + 2$. From (38) and (39), we obtain the following formulae of the coefficients of $\tilde{h}_{N,1}$ (or $\tilde{h}_{N,2}$) for a given h_N:

$$\begin{cases} \tilde{h}_{N,1}(2m) = \sqrt{2}\delta_{m0} - h_N(1-2m) \\ \tilde{h}_{N,1}(2m+1) = \dfrac{1}{\sqrt{2}}\delta_{m0} \end{cases} \quad \text{for } N \text{ is odd} \tag{47}$$

and (48), shown at the bottom of the page.

$$\begin{cases} \tilde{h}_{N,2}(2m) = \sqrt{2}\delta_{m0} - \dfrac{1}{2\sqrt{2}}(h_N(-1-2m) + h_N(1-2m)) \\ \tilde{h}_{N,2}(2m-1) = \dfrac{1}{2\sqrt{2}}(\delta_{m0} + \delta_{m1}) \end{cases} \quad \text{for } N \text{ is even} \tag{48}$$

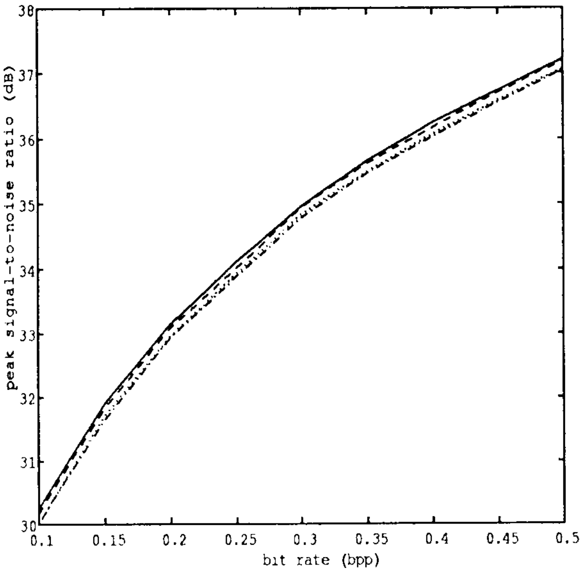

(a)

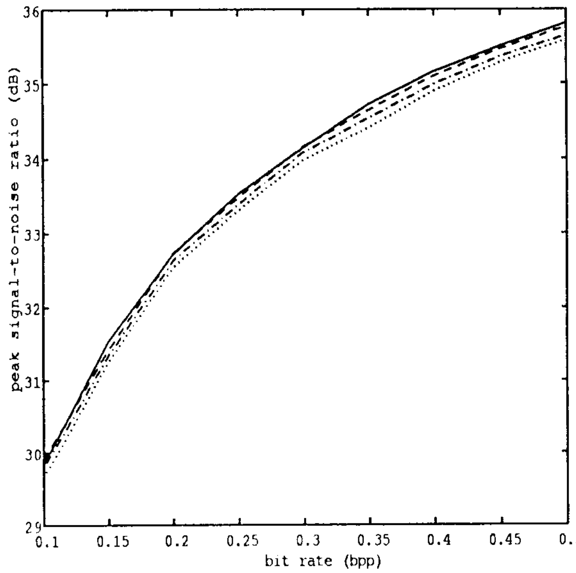

(b)

Fig. 2. Image compression performance (solid line: CDF-9-7; dash-dotted line: GBCW-9-7; dashed line: GBCW-13-7; dotted line: GBCW-13-11). (a) Lenna. (b) Peppers.

One useful property of the MLBCW system is that both h_N and $\tilde{h}_{N,\tilde{N}}$ have about half of their coefficients that are zero-valued.

G. Strict Biorthogonal Coifman Wavelet Systems

Now we consider another special class of the GBCW systems in which the degree of vanishing moments for ψ is equal to those of $\tilde{\phi}, \tilde{\psi}$, and ϕ, i.e., all four functions have the same degree of vanishing moments. This subclass of the GBCW systems was originally introduced in [11].

Definition 8: A GBCW system of order N is called a *strict biorthogonal Coifman wavelet* system (SBCW system) of order N if the degree of vanishing moments for ψ is also N, i.e., $\tilde{N} = N$.

From (38) and (39), we obtain the following formulae of the coefficients of $\tilde{h}_{N,N}$ for a given h_N:

$$\begin{cases} \tilde{h}_{N,N}(2m+1) = h_N(2m+1) \\ \tilde{h}_{N,N}(2m) = \sqrt{2}\left(\delta_{m0} - \sum_l h_N(2l+1)h_N(2l+1-2m)\right). \end{cases} \tag{49}$$

It is straightforward to check that $\tilde{h}_{N,N}(2m) = \tilde{h}_{N,N}(-2m), \forall m$ and $\forall N$.

III. Performance Evaluation of Three GBCW Systems for Image Transform Coding

We show that the FB's corresponding to the symmetric GBCW systems are very suited to image transform coding. The GBCW systems of orders one and two are the same as the biorthogonal spline wavelet systems of the same order [2], in which there are a few short FB's that have been shown to have good compression capability [7]. We propose that three pair of dual filters, $\{\tilde{h}_{4,2}, h_4\}$ of 9-7 taps, $\{\tilde{h}_{4,4}, h_4\}$ of 13-7 taps, and $\{\tilde{h}_{6,2}, h_6\}$ of 13-11 taps (we refer to them as GBCW-9-7, GBCW-13-7, and GBCW-13-11, respectively) in the family of GBCW systems have remarkable compression potential. We mainly compare them with the widely used CDF-9-7 FB. We apply some image-independent measures as well as some image-dependent measures to systematically compare these four FB's for image transform coding.

A. Image-Independent Measures

In [7], several image-independent measures based on some properties of the dual filters have been recommended to evaluate wavelet systems for image transform coding. We list the comparison results using these measures in Table II.

1) Regularity: It has been well known that the regularity of wavelet systems is only partially related to the quality of reconstructed images via wavelet transform coding [3], [7], [20]. However, for short wavelet filters, regularity is still closely related to the compression performance [20]. We use the algorithm by Rioul [21] to estimate Hölder regularity from dual filters. Usually, smoothness of the synthesis scaling function ϕ is more important than that of the analysis scaling function $\tilde{\phi}$ in determining the quality of a reconstructed image, and the latter is more relevant to energy compaction capability than the former for smooth images. Therefore, there is a tradeoff between these two factors when choosing short wavelet FB's. The comparison results in Table II indicate that the GBCW-13-7 FB and the CDF-9-7 FB are better than the other two FB's in terms of the distribution of regularity.

2) Shift-Variant Impulse Response: The impulse response of an J-level combined subband analysis/synthesis system formed by a pair of dual filters h and $\tilde{h}$ [7] is defined as

$$f_{h,\tilde{h},J}(n, n_0) = \mathcal{R}_{h,\tilde{h},J}\{W_J(n)\mathcal{D}_{h,\tilde{h},J}\{\delta(n-n_0)\}\} \tag{50}$$

where $\delta(n-n_0)$ is an impulse at $n = n_0$; $\mathcal{D}$ and $\mathcal{R}$ are the wavelet decomposition and reconstruction operators, respec-

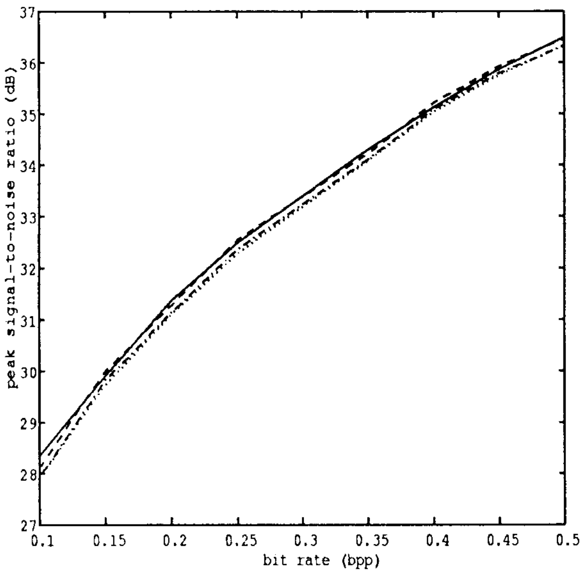

(a)

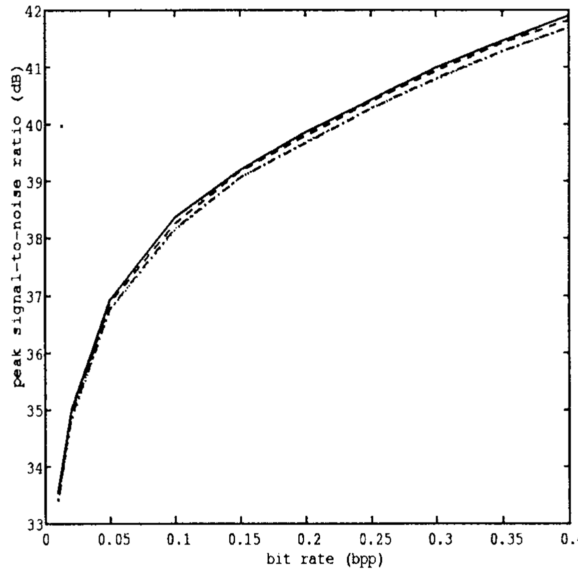

(b)

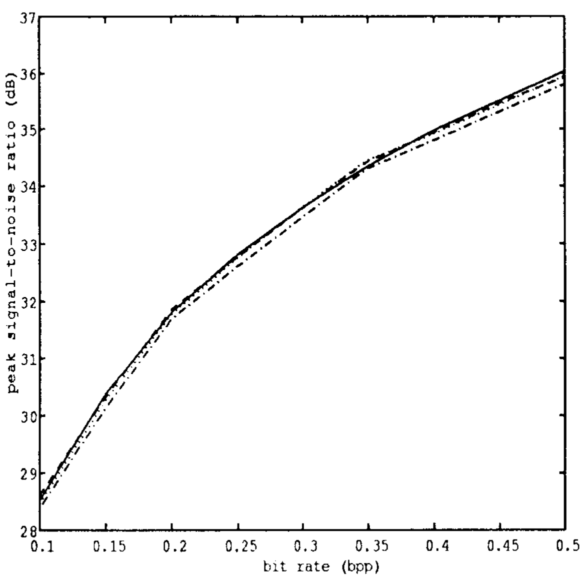

(c)

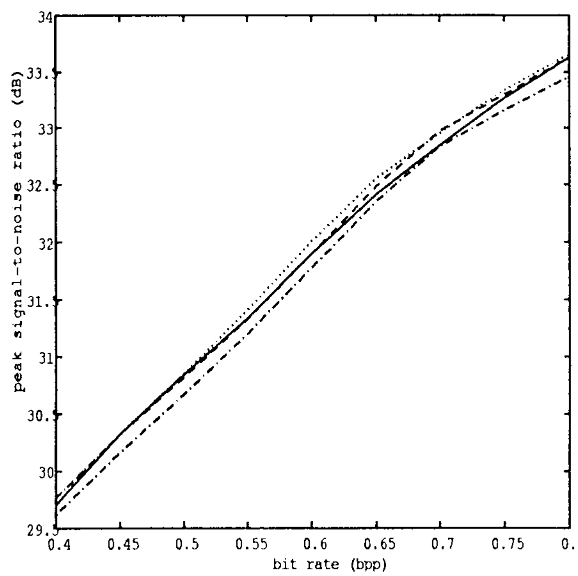

(d)

Fig. 3. Image compression performance (solid line: CDF-9-7; dash-dotted line: GBCW-9-7; dashed line: GBCW-13-7; dotted line: GBCW-13-11). (a) Boats. (b) Building. (c) Fingerprint-1. (d) Fingerprint-2.

tively; and the wavelet transform domain indicator function W_J is defined as $W_J(n) = 1$ if $n \in \mathbb{L}$ and $W_J(n) = 0$ otherwise, where $\mathbb{L}$ is the set of indices for the subband signal with the lowest resolution. Since the biorthogonal DWT is shift-variant, the impulse response defined above also depends on the location of the impulse. Unlike [7], we here use both the minimum and the average peak-to-sidelobe ratio (MPSR and APSR) in dB among the 2^J possible impulse responses in an J-level DWT/IDWT to characterize both the worst-case and the average oscillatory behavior, or the ringing effect, in the system response, which usually results in visually annoying artifacts in reconstructed images. The higher MPSR and APSR correspond to the weaker ringing behavior.

We choose $J = 3$ in our experiments. From Table II, we can see that the APSR's of the GBCW-9-7 FB and the GBCW-13-11 FB are better than those of the other two FB's, while the MPSR's of the latter two FB's are better than those of the former two FB's.

3) Shift-Variant Step Response: Since the ringing artifact often occurs near the regions of edges in reconstructed images, it may also be characterized by both the maximum and the average fractional overshoot of the second sidelobe (MFOSS and AFOSS) among the 2^L possible step responses of the combined analysis/synthesis system (defined in a similar way to impulse response), which are closely related to the worst-case and the average ringing effect, respectively. Strong overshoots in the step responses will lead to significant ringing in the reconstructed image [7].

The comparison results in Table II indicate that the GBCW-9-7 FB has much lower AFOSS than the other three FB's, while the GBCW-9-7 FB and the GBCW-13-7 FB are better than the other two FB's in terms of the MFOSS.

From the above comparison of the impulse responses and the step responses for the four FB's, we can expect that the GBCW-9-7 FB and the GBCW-13-7 FB will exhibit weaker ringing artifact than the other two FB's.

B. Image-Dependent Measures

The energy compaction is one of the most important metrics in the evaluation of filters used in transform coding schemes. However, to our knowledge, there is no measure for energy compaction that can be used independent of images. We choose six test images: Lenna (512 $\times$ 512), peppers (512 $\times$ 512), boats (576 $\times$ 720), building (a synthetic aperture radar image, 800 $\times$ 800), fingerprint-1 (768 $\times$ 768) and fingerprint-2 (480 $\times$ 384), which are all 256 gray-level images.

1) Weighted Subband Coding Gain: For a given image X of size M and a subband decomposition scheme, which decomposes X into K subband images: $X_0, X_1, \cdots, X_{K-1}$, the energy compaction property of the FB can be characterized by *weighted subband coding (SBC) gain* (see [22] for detailed discussion on coding gain)

$$G_{\text{SBC}} = C_X \sigma_X^2 \prod_{k=0}^{K-1} \left(\left(\frac{M}{M_k} \right) w_k \sigma_{X_k}^2 \right)^{-M_k/M} \tag{51}$$

where C_X is a constant related to the image X, M_k is the size of the subband image X_k, σ_X^2, and $\sigma_{X_k}^2$ are the variances of the image X and the subband image X_k, respectively, and w_k is the weight for the subband image X_k, which takes into consideration the different energy contributions from different subbands due to the nonorthogonality of the transform. We apply the method proposed in [23] to compute these filter-related weights $\{w_k\}$, and here we also propose a new formula that generalizes the simple cases in [23]. Assume that the synthesis channel for the subband image X_k consists of J_k filters in the horizontal direction, in the order of $u_{k,1}, u_{k,2}, \cdots, u_{k,J_k}$, and J_k filters in the vertical direction, in the order of $v_{k,1}, v_{k,2}, \cdots, v_{k,J_k}$ (here we consider only the two-dimensional separable FB's). The weight w_k is then given by

$$w_k = 2^{-2J_k} \left(\sum_n |\overline{u}_k(n)|^2 \right) \left(\sum_n |\overline{v}_k(n)|^2 \right) \tag{52}$$

where the z-transforms of $\overline{u}_k$ and $\overline{v}_k$ are respectively given by

$$\overline{U}_k(z) = \prod_{m=1}^{J_k} U_{k,m}(z^{2^{J_k - m}}) \quad \text{and}$$
$$\overline{V}_k(z) = \prod_{m=1}^{J_k} V_{k,m}(z^{2^{J_k - m}}). \tag{53}$$

From (51), one can see that SBC gain depends strongly on image content. It is also partially theoretical, because the definition of SBC gain is based on some assumptions that are not always valid in practice. However, due to the lack of better metrics to measure energy compaction capability, the SBC gain is still widely used.

Fig. 4. Original Lenna image.

The experimental results are given in Table III. We find that the SBC gains of GBCW-13-7 FB are slightly better than those of the other three FB's for the first four images, and the SBC gains of the three GBCW FB's are better than those of the CDF-9-7 FB for the two fingerprint images.

2) Simulation of Image Transform Coding: We apply the wavelet transform coding algorithm proposed in [24], which is one of the state-of-the-art algorithms for still image compression, to test the rate-distortion performance of the four FB's. The rate and the distortion are measured by bit rate in bits per pixel and peak signal-to-noise ratio (PSNR) in dB, respectively. The simulation results in Figs. 2 and 3 indicate that the four FB's have very close performance over a wide range of compression ratios. For the first four images, the GBCW-13-7 FB is as good as the CDF-9-7 FB, which is slightly better than the other two FB's. However, for the fingerprint images, the GBCW-13-7 FB and the GBCW-13-11 FB are a bit better than the CDF-9-7 FB in the range of medium bit rates, as indicated by the comparison results of their SBC gains.

We use the Lenna image to compare the perceptual quality of the images coded by the four FB's. In order to display various coding artifacts, we choose a high compression ratio 80 : 1. Figs. 4 and 5, respectively, depict the original Lenna image and four coded versions. While the global visual qualities of all four images in Fig. 5 are fairly close, there are a few locally distinct distortions. The edges in Fig. 5(b) are slightly sharper than those in the other three images. Fig. 5(b) and 5(c) exhibit slightly less ringing in the smooth regions around sharp edges than the other two, which is indeed predicted by our study of their shift-variant impulse responses and step responses. Fig. 5(b) maintains a bit more textures than the other three, e.g. the stripes on the hat. This and the result that the GBCW-13-7 FB performs well in coding fingerprint images may suggest that it is more suitable for compression of texture images. We also note that the bright small dot to the left of the

(a)

(b)

(c)

(d)

Fig. 5. Coded Lenna images at 0.1 b/pixel (compression ratio 80 : 1) by: (a) CDF-9-7 (30.23 dB); (b) GBCW-13-7 (30.16 dB); (c) GBCW-9-7 (30.01 dB); (d) GBCW-13-11 (30.00 dB).

hat in Fig. (4) is well preserved in Fig. 5(b)–(d) but severely blurred in Fig. 5(a), which indicates that the three GBCW FB's preserve the intensity of impulses better than the CDF-9-7 FB does. Therefore, we conclude that even though Fig. 5(a) has the highest PSNR, Fig. 5(b) shows the best perceived quality, and the other two images are perceptually almost as good as Fig. 5(a) though their PSNR's are more than 0.2dB lower than that of Fig. 5(a).

Having completed this work, the authors learned that the comparison between the CDF-9-7 FB and the GBCW-9-7 FB was also performed using different coding algorithms in [17, pp. 249] and [18]. Their results are similar to ours: while the CDF-9-7 FB has slight advantage in terms of PSNR and maximum error, the GBCW-9-7 FB results in perceptually better image quality.

C. Computational Complexity

It is well known that DWT/IDWT of a length-M signal have $O(M)$ computational complexity if the lengths of the dual filters used in the transformation are relatively short compared to M. However, the constants in the $O(M)$ representation can be quite different for different wavelet systems used in the transformation. The following proposition gives in general the

TABLE IV
COMPARISON OF THE COMPUTATIONAL COMPLEXITIES IN TERMS OF THE AVERAGE NUMBER OF OPERATIONS REQUIRED TO COMPUTE EACH COEFFICIENT IN THE TRANSFORMATION (THE SYMBOLS "$\times$," "$+$," AND "$\times 2^b$" STAND FOR FLOATING-POINT MULTIPLICATION, FLOATING-POINT ADDITION, AND MULTIPLICATION BY 2^b, RESPECTIVELY)

	Operation	CDF-9-7	GBCW-9-7	GBCW-13-7	GBCW-13-11
DWT	$\times$	4.5	0	0	0
	$+$	7	6.5	10.5	13
	$\times 2^b$	0	3	4.5	5.5
IDWT	$\times$	4.5	0	0	0
	$+$	7	6	10.5	11.5
	$\times 2^b$	0	3	5	4.5

computational complexity of the DWT and the IDWT using a symmetric biorthogonal system.

Proposition 9: For a length-M one-dimensional, real-valued signal, a symmetric analysis lowpass filter of length $\tilde{L}$, and a symmetric synthesis lowpass filter of length L, the numbers of floating-point additions required in a J-level DWT and a J-level IDWT are given, respectively, by

$$A_{\mathrm{DWT}} = \begin{cases} C_{M,J}(L+\tilde{L}-2)/2 \\ \quad \text{for } L \text{ and } \tilde{L} \text{ are odd} \\ C_{M,J}(\max(L,\tilde{L})+L+\tilde{L}-4)/4 \\ \quad \text{for } L \text{ and } \tilde{L} \text{ are even} \end{cases} \tag{54}$$

and

$$A_{\mathrm{IDWT}} = C_{M,J}(L+\tilde{L}-2)/2. \tag{55}$$

The numbers of floating-point multiplications required in a J-level DWT and a J-level IDWT are identical and given by

$$M_{\mathrm{DWT}} = M_{\mathrm{IDWT}} = C_{M,J}(\lceil L/2\rceil + \lceil \tilde{L}/2\rceil)/2 \tag{56}$$

where $C_{M,J}$ is the number of coefficients needed to be computed in the transformation and given by $C_{M,J} = 2M(1-2^{-J})$, where we assume for simplicity that M is a multiple of 2^J. Obviously, the quantity $C_{M,J}$ only depends on the length of the signal and the number of decomposition/reconstruction levels, and does not depend on the dual filters.

The proof of the above proposition is straightforward. According to Proposition 9, the computational complexity of the DWT/IDWT using the CDF-9-7 FB, whose coefficients are all irrationals, is exactly determined by those formulae. For the GBCW FB's, we can apply a multiplication-free scheme for DWT/IDWT, where the most computationally costly operations, floating-point multiplications, are replaced by the computationally cheap operations, multiplications of 2^b or binary shifts, at the cost of a reasonable increase in the number of floating-point additions. In addition, some useful properties of the GBCW FB's can be applied to further reduce the complexity. For instance, all the coefficients of the three discussed GBCW FB's are very close to some dyadic numbers so that the increases of floating-point additions are small.

The special properties of the GBCW FB's lead to the flexibility of implementations of the multiplication-free DWT/IDWT, which results in slightly different computational complexities. In our implementations, the numbers of floating-point additions are minimized. We lists the resulted computational complexities corresponding to the three GBCW FB's, as well as that of the GBCW-9-7 FB, in Table IV. If the original image data are integers, then the DWT will be even faster, because the multiplications by 2^b can be implemented as using the binary shift operations. Therefore, the total computational costs of the DWT/IDWT using the three GBCW FB's are smaller than using the CDF-9-7 FB.

It might be interesting to combine the proposed multiplication-free algorithm with other fast wavelet transform algorithms (e.g. the lifted fast wavelet transform [5]), which may lead to computationally more efficient algorithms. In addition, the following question might be a topic of future research: for a certain biorthogonal wavelet system with dyadic filter coefficients, which implementation is optimal in terms of computational complexity?

IV. CONCLUSIONS

We have presented the design of a novel class of biorthogonal wavelet systems, the GBCW systems, which possess several remarkable properties. In particular, three FB's in this family have been shown to be competitive with the CDF-9-7 FB in DWT-based image compression. Furthermore, the multiplication-free DWT/IDWT using the GBCW systems are promising in the realization of real-time image and video codec. Therefore, we feel that these GBCW systems are serious candidates for the choice of wavelet systems in current and future image/video transform coding standards.

ACKNOWLEDGMENT

The authors wish to thank the three anonymous reviewers for their careful review and insightful comments that helped us improve the paper. In particular, the authors gratefully acknowledge the first reviewer for pointing out some related work.

REFERENCES

[1] I. Daubechies, *Ten Lectures on Wavelets.* Philadelphia, PA: SIAM, 1992.
[2] A. Cohen, I. Daubechies, and J. C. Feauveau, "Biorthogonal bases of compactly supported wavelets," *Commun. Pure Appl. Math.*, vol. 45, pp. 485–560, 1992.
[3] M. Vetterli and C. Herley, "Wavelets and filter banks: Theory and design," *IEEE Trans. Acoust., Speech, Signal Processing*, vol. 40, pp. 2207–2232, Sept. 1992.
[4] S.-M. Phoong, C. W. Kim, P. P. Vaidyanathan, and R. Ansari, "A new class of two-channel biorthogonal filter banks and wavelet bases," *IEEE Trans. Signal Processing*, vol. 43, pp. 649–665, Mar. 1995.
[5] W. Sweldens, "The lifting scheme: A custom-design construction of biorthogonal wavelets," *Appl. Comput. Harmon. Anal.*, vol. 3, pp. 186–200, 1996.
[6] Fed. Bureau Invest., "The FBI wavelet/scalar quantization fingerprint image compression standard."
[7] J. D. Villasenor, B. Belzer, and J. Liao, "Wavelets filter evaluation for image compression," *IEEE Trans. Image Processing*, vol. 4, pp. 1053–1060, Aug. 1995.
[8] H. Tao and R. J. Moorhead, "Lossless progressive transmission of scientific data using biorthogonal wavelet transform," in *Proc. IEEE Int. Conf. Image Processing*, Austin, TX, Nov. 1994, vol. III, pp. 373–377.
[9] G. Beylkin, R. Coifman, and V. Rokhlin, "Fast wavelet transforms and numerical algorithms," *Commun. Pure Appl. Math.*, vol. 44, pp. 141–183, 1991.
[10] I. Daubechies, "Orthonormal bases of compactly supported wavelets II—Variations on a theme," *SIAM J. Math. Anal.*, vol. 24, pp. 499–519, Mar. 1993.
[11] J. Tian and R. O. Wells, Jr., "Vanishing moments and wavelet approximation," Tech. Rep. CML TR95-01, Computat. Math. Lab., Rice Univ., Houston, TX, Jan. 1995.

[12] I. Daubechies, "Orthonormal bases of compactly supported wavelets," *Commun. Pure Appl. Math.*, vol. 41, pp. 909–996, 1988.
[13] G. Deslauriers and S. Dubuc, "Symmetric iterative interpolation process," *Constr. Approx.*, vol. 5, pp. 49–68, 1989.
[14] R. Ansari, C. Guillemot, and J. F. Kaiser, "Wavelet construction using Lagrange halfband filters," *IEEE Trans. Circuits Syst.*, vol. 38, pp. 1116–1118, Sept. 1991.
[15] M. J. Shensa, "The discrete wavelet transform: Wedding the à trous and Mallat algorithms," *IEEE Trans. Signal Processing*, vol. 40, pp. 2464–2482, Oct. 1992.
[16] N. Saito and G. Beylkin, "Multiresolution representation using the autocorrelation functions of compactly supported wavelets," *IEEE Trans. Signal Processing*, vol. 41, pp. 3584–3590, Dec. 1993.
[17] G. Strang and T. Nguyen, *Wavelets and Filter Banks*. Wellesley, MA: Wellesley-Cambridge, 1996.
[18] G. Strang, "Creating and comparing wavelets," in *Numerical Analysis: A. R. Mitchell Birthday Volume*, G. A. Watson and D. F. Griffiths, Eds. Singapore: World Scientific, 1996.
[19] O. Rioul and P. Duhamel, "Fast algorithms for discrete and continuous wavelet transforms," *IEEE Trans. Inform. Theory*, vol. 38, pp. 569–586, Mar. 1992.
[20] O. Rioul, "Regular wavelets: A discrete-time approach," *IEEE Trans. Signal Processing*, vol. 41, pp. 3572–3579, Dec. 1993.
[21] ———, "Simple regularity criteria for subdivision schemes," *SIAM J. Math. Anal.*, vol. 23, pp. 1544–1576, Nov. 1992.
[22] N. S. Jayant and P. Noll, *Digital Coding of Waveforms*. Englewood Cliffs, NJ: Prentice-Hall, 1984.
[23] J. W. Woods and T. Naveen, "A filter based bit allocation scheme for subband compression of HDTV," *IEEE Trans. Image Processing*, vol. 1, pp. 436–440, July 1992.
[24] A. Said and W. A. Pearlman, "A new, fast, and efficient image codec based on set partitioning in hierarchical trees," *IEEE Trans. Circuits Syst. Video Technol.*, vol. 6, pp. 243–250, June 1996.

Dong Wei (S'94) was born in Beijing, China, in 1968. He received the B.Eng. degree from the Department of Automation, Tsinghua University, Beijing, in 1992, and the M.S. degree in electrical engineering from Rice University, Houston, TX, in 1995. He is currently pursuing the Ph.D. degree in electrical engineering at the University of Texas, Austin.

From 1992 to 1993, he was a Software Engineer at Tsinghua University. From 1993 to 1995, he was a Research Assistant in the Digital Signal Processing Group and the Computational Mathematics Laboratory at Rice University. From 1995 to 1996, he held a part-time research fellowship at Schlumberger Austin Research, Austin, TX. Since 1995, he has been a Research Assistant at the Laboratory for Vision Systems, University of Texas. His current research interests include wavelet theory and its applications, time-frequency/time-scale representations, image and video compression, and signal and image enhancement.

Jun Tian, photograph and biography not available at the time of publication.

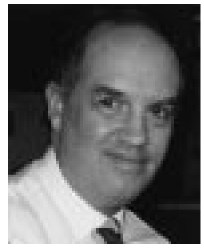

Raymond O. Wells, Jr. received the undergraduate degree in mathematics from Rice University, Houston, TX, and the Ph.D. degree from the Courant Institute of Mathematical Sciences, New York University, New York, NY.

He has been on the faculty of Rice University since 1965, and is currently Professor of mathematics and education, Director of the Computational Mathematics Laboratory, and Director of the Rice University School of Mathematics Project. He has been a Visiting Member at the Institute for Advanced Study, and a Visiting Professor at Brandeis University, University of Göttingen, and the University of Colorado at Boulder. Most recently, he has been involved with efforts to build a bridge between the Rice mathematical sciences faculty and the Houston area mathematics teachers and with the development of the Computational Mathematics Laboratory at Rice, a mathematics laboratory collaboration involving various mathematical scientists and engineers. His research interests have been in several complex variables, algebraic and differential geometry, mathematical physics, applied mathematics, and mathematics education. His current research efforts concern wavelet theory and its application in a variety of areas of numerical analysis and signal processing.

Dr. Wells is the recipient of Fulbright, Guggenheim, and Alexander von Humboldt awards, and is a Fellow of the AAAS.

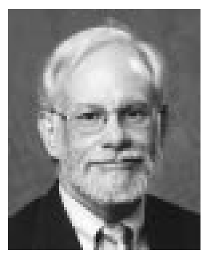

C. Sidney Burrus (S'55–M'61–SM'75–F'81) was born in Abilene, TX, on October 9, 1934. He received the B.A., B.S.E.E., and M.S. degrees from Rice University, Houston, TX in 1957, 1958, and 1960, respectively, and the Ph.D. degree from Stanford University, Stanford, CA, in 1965.

From 1960 to 1962, he taught at the Navy Nuclear Power School, New London, CT, and during the summers of 1964 and 1965 he was a Lecturer in Electrical Engineering at Stanford University. In 1995, he joined the faculty at Rice University, where he is now the Maxfield and Oshman Professor of Electrical and Computer Engineering and Director of the Computer and Information Technology Institute. From 1972 to 1978, he was Master of Lovett College, Rice University, and from 1984 to 1992, he was Chairman of the Electrical and Computer Engineering Department at Rice. From 1975 to 1976 and again from 1979 to 1980, he was a Guest Professor at the Universitaet Erlangen-Nuernberg, Germany. During the summer of 1984, he was a Visiting Fellow at Trinity College, Cambridge University, U.K., and during the academic year 1989–1990 he was a Visiting Professor at the Massachusetts Institute of Technology, Cambridge.

Dr. Burrus is a member of Tau Beta Pi and Sigma Xi. He has received teaching awards at Rice in 1969, 1974, 1976, 1980, and 1989, an IEEE S-ASSP Senior Award in 1974, a Senior Alexander von Humboldt Award in 1975, and a Senior Fulbright Fellowship in 1985. He was a Distinguished Lecturer for the Signal Processing Society and for the Circuits and Systems Society from 1989 through 1992, and received the Signal Processing Society Award in 1995. He served on the IEEE S-SP ADCOM for three years and has co-authored five books on digital signal processing.